DETERMINING THE IMPACT OF CALCIUM-ATPASE ACTIVITY IN HYPERSTIMUALTED *C. ELEGANS* MUSCLES

by

Allison N. Davis

A thesis submitted to the Faculty of the University of Delaware in partial fulfillment of the requirements for the degree of Honors Degree in Major with Distinction

Spring 2022

DETERMINING THE IMPACT OF CALCIUM-ATPASE ACTIVITY IN HYPERSTIMUALTED *C. ELEGANS* MUSCLES

by

Allison N. Davis

Approved: _____

Jessica Tanis, PhD
Professor in charge of thesis on behalf of the Advisory Committee

Approved: _____

Gary Laverty, PhD
Committee member from the Department of Department Name

Approved: _____

Carlton Cooper, PhD
Committee member from the Board of Senior Thesis Readers

Approved: _____

Michael Chajes, Ph.D
Dean, University Honors Program

ACKNOWLEDGMENTS

I feel honored to have been supported by so many people throughout my undergraduate research experience. I'd especially like to thank Dr. Tanis for her incredible guidance and mentorship throughout my time in the lab. Her incredible dedication to fostering a collaborative work environment and encouraging critical analysis have tremendously affected my academic, professional, and personal life. Thank you to my current lab members: Andy Lam, Michael Clupper, Malek Elsayyid, Denis Touroutine, Rachael Gill, Ime Nkanta, Emylee Kerslake, Karli Sunnergren, Carter O'Brien, John Salsini -Tobias, Katherine Wagner, Rachel Wang, and Vasilios Lomas. A special thank you to Erin Smith for training me in the Tanis lab and Andy Lam for answering every random question I have. Thank you to the Milton Stetson Family and Honors College for funding me outside of traditional semesters, allowing me to continue doing this research that I love. I'd also like to thank the Undergraduate Research Office for giving me the resources and guidance necessary to complete this thesis. Thank you to my thesis committee: Dr. Jessica Tanis, Dr. Gary Laverty, and Dr. Carlton Cooper, for their dedicating their time and support. Finally, I'd like to thank my friends and family for their tireless support through this entire research process, even though they usually had no idea what I was talking about.

TABLE OF CONTENTS

LIST OF TABLES

LIST OF FIGURES

ABSTRACT

Calcium-ATPases are vital pumps in the plasma membrane and sarcoplasmic reticulum that are required for removal of calcium (Ca^{2+}) against the concentration gradient to maintain low intracellular Ca^{2+}. At the neuromuscular junction (NMJ), binding of the excitatory neurotransmitter acetylcholine (ACh) to postsynaptic receptors leads to an increase in intracellular Ca^{2+} and muscle contraction. Reducing intracellular Ca^{2+} after muscle contraction is required to enable relaxation. As in vertebrate skeletal muscle, activation of ACh receptors (AChRs) on the body wall muscles of the model organism *C. elegans* cause muscle contraction. A genome wide RNAi screen for altered sensitivity to the AChR agonist levamisole showed that loss of MCA-3, a plasma membrane Ca^{2+}-ATPase (PMCA), resulted in a levamisole resistant phenotype. This suggests that another mechanism is more efficient in reducing intracellular Ca^{2+} when MCA-3 is not present. SCA-1 is a sarcoplasmic reticulum Ca^{2+}-ATPase (SERCA) in *C. elegans* body wall muscles. SERCAs move two Ca^{2+} for every molecule of ATP, while PMCAs are less efficient and move one Ca^{2+} for every molecule of ATP. When cellular ATP is low, Ca^{2+} cannot be pumped out of the cytoplasm and the muscles remain contracted. I hypothesize that mutation of each gene individually will cause altered phenotype and paralysis rates due to the difference in ATP utilization. I performed behavioral assays to determine levamisole induced phenotypes. *sca-1* mutation and RNAi knockdown resulted in a significant levamisole hypersensitive phenotype.

Next, I looked to investigate the molecular causes of the observed paralysis. ATP levels were quantified in RNAi knockdown animals after 0, 30, and 60 minutes of levamisole treatment. *sca-1* knockdown depleted ATP significantly over the first 30 minutes, while ATP depletion in the *mca-3* knockdown did not occur until the last 30 minutes of levamisole treatment. Finally, I conducted imaging tracking intracellular Ca^{2+} using LSM880 confocal microscopy. I optimized imaging methods and parameters that show promise for future investigation of mutants and RNAi knockdowns. In conclusion, SCA-1 plays an important role in reducing intracellular Ca^{2+}, and ATP availability plays a role in levamisole paralysis rate.

Chapter 1

Introduction

1.1 Neuromuscular Junction

The neuromuscular junction (NMJ) is described as the synapse between a motor neuron and muscle. Activation of postsynaptic ionotropic acetylcholine receptors (AChRs) on skeletal muscle results in an electrical signal that leads to muscle contraction (Taylor and Brown 1999; Rand 2007). Disruption of neuromuscular function results in myasthenic syndromes and muscular dystrophies in humans, making it an important area of study. The nematode *C. elegans* has been used extensively used to learn about evolutionarily conserved fundamental biological processes and mechanisms of disease.

Presynaptically, acetylcholine (ACh) is formed by the combination of acetyl coenzyme A and choline. When a motor neuron is activated, the resulting depolarization effect opens voltage gated calcium channels (Ca^{2+}). The resulting influx of calcium results in release of ACh-filled synaptic vesicles into the synaptic cleft (Taylor and Brown 1999; Rand 2007). Once in the synaptic cleft, ACh binds to the alpha subunit of the ionotropic AChR on the postsynaptic muscle. The channel opens allowing for an influx of sodium (Na^{+}) which causes depolarization (Rand 2007; Brown *et al*. 2006). This results in activation of the ryanodine receptor which releases

Ca^{2+} from the sarco-endoplasmic reticulum into the cytoplasm (Robertson *et al.* 2010; Liu *et al.* 2011). The increase in Ca^{2+} abundance enables Ca^{2+} to bind to troponin, causing tropomyosin to shift. This shift allows myosin and actin to bind to each other, causing muscle contraction (Clapham 2007). To stop muscle contraction, sarco-endoplasmic reticulum Ca^{2+}- ATPases (SERCA) pump Ca^{2+}out of the cytoplasm and back into the intracellular stores of the sarcoplasmic reticulum. Any remaining ACh left in the synaptic cleft is hydrolyzed by acetylcholinesterase (AChE) into choline and acetic acid (Trang and Khandhar 2020).

The *C. elegans* body-wall muscles (BWMs) control *C. elegans* motion and are functionally comparable to vertebrate skeletal muscle. In mammals, axons from the presynaptic neuron extend to synapse onto the postsynaptic muscle. However, *C. elegans'* neurons are unipolar. This means that they only have a single process that has different segments for releasing and receiving signals. BWMs extend muscle arms out connecting toward motor neurons, and the postsynaptic receptors are clustered on these muscle arms. Locomotion is controlled by signaling through ACh and GABA receptors which allow muscles on one side of the *C. elegans* body to contract while muscles on the other side relax, enabling coordinated body bends (Richmond and Jorgenson 1999).

1.2 *Caenorhabditis elegans*

C. elegans is a completely harmless soil-dwelling nematode. *C. elegans* has two sexes, hermaphrodites and males, which are morphologically distinct. *C. elegans* with

one X chromosome (X0) are males. Males make sperm in a gonad that has one reflexed arm that exits at the back. The male tail is an elaborate but highly ordered structure that is used in mating with hermaphrodites. *C. elegans* with two X chromosomes (XX) are hermaphrodites. Hermaphrodites have a two-armed gonad that bends around the vulva in the middle of the animal. Hermaphrodites are morphologically identical to females in related species. In *C. elegans*, when meiosis begins, the hermaphrodite makes sperm for about an hour—about 150 sperm in each arm of the gonad. Then spermatogenesis shuts off and oogenesis begins and continues for the remainder of the worm's fertile life. A hermaphrodite can mate with a male, in which case the male sperm are used in fertilization. If no males are provided, a hermaphrodite will use her own sperm to fertilize her own ova; hermaphrodites cannot fertilize each other (Riddle *et al*. 1997; Singson 2001).

After fertilization, an eggshell forms around the egg and mitotic divisions begin. Depending on conditions, an egg will be laid about two hours or later after fertilization. The worm hatches from the egg at about twelve hours, having completed embryogenesis. The recently hatched worm, termed an L1, is barely visible. It will grow to become an L2, and then an L3 and L4. The final molt is from an L4 to an adult hermaphrodite, which begins laying eggs twelve hours later (Riddle *et al*. 1997; Singson 2001).

Overall, *C. elegans* are an ideal model organism of study. *C. elegans* are transparent, making them ideal for internal visual observations, as well as fluorescent protein-tagged imaging. Another benefit of *C. elegans* study is their short generation

time. The life cycle takes about three days at 25℃ and extends to 4 days at 15℃ (Brenner 1974). A hermaphrodite will lay about four eggs an hour for about 72 hours (when she runs out of sperm) but will live for weeks after she has stopped laying eggs (Riddle *et al*. 1997; Singson 2001). *C. elegans* also have a large brood size. Each adult can have between 300 and 1,000 progeny depending on the strain (Corsi 2007). This large number of progeny is ideal for many behavioral and quantitative assays. Finally, their simple neuroanatomy and functionally equivalent muscular system makes *C. elegans* ideal for neuromuscular junction research.

1.3 Levamisole Function

Levamisole is an anthelmintic agent that binds to and constitutively activates the levamisole sensitive class of AChRs (L-AChRs) on the body wall muscles, resulting in time dependent paralysis (Richmond and Jorgensen 1999; Lewis *et al.* 1980). Levamisole binding to L-AChRs causes an influx of Ca^{2+}, depolarization, and muscle contraction. Animals will remain paralyzed, in a rodlike shape, while in the presence of levamisole and eventually die if levamisole exposure persists (Galimov *et al.* 2018; Chaya *et al.* 2021). Altered sensitivity to levamisole has been used to identify *C. elegans* with defects in postsynaptic cholinergic signaling and muscle function (Lewis *et al.* 1980; Gally *et al.* 2004; Chaya *et al.* 2021).

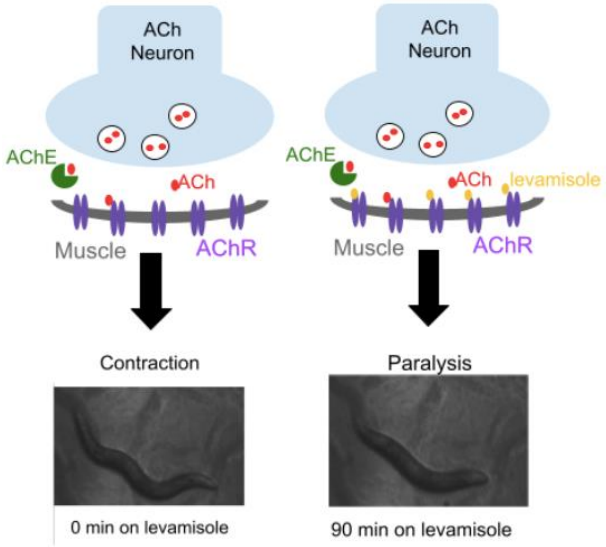

Figure 1: Levamisole Effect on *C. elegans*

ACh is released from the motor neuron and binds to AChRs on the muscle, resulting in muscle contraction. Levamisole is a L-AChR agonist that causes constitutive L-AChR activation, leading to paralysis.

Hypersensitivity or resistance to levamisole has been traditionally assessed by transferring animals to agar plates containing levamisole and then regularly prodding the worms to determine the time point at which paralysis occurs, however the liquid levamisole swim assays, developed by members of the Tanis lab, eliminate the need for physical manipulation of the animals and allows for screening of hundreds of animals in just one hour. There are several key genes that are known to impact levamisole induced paralysis. *unc-29* encodes the alpha subunit of the L-AChR. This subunit has been found to be necessary for L-AChR function and is expressed in the head and body wall muscles (Fleming *et al*. 1997). The alpha subunit of the L-AChR

binds acetylcholine and allows for subsequent depolarization of the body wall muscles (Figure 2). This receptor also binds levamisole, leading to constitutive depolarization, leading to paralysis (Martin *et al.* 2012). *unc-29* mutation causes a levamisole resistance phenotype, as loss of the L-AChR prevents depolarization .(Fleming *et al.* 1997). Additionally, *egl-19* encodes for an L-type voltage gated Ca^{2+}channel. This voltage gated Ca^{2+} channel is opened following local depolarization induced by activation of the L-AChR. This allows for an influx of Ca^{2+}, which ultimately binds to the ryanodine receptor UNC-68. UNC-68 releases Ca^{2+} stores from the sarcoplasmic reticulum to further contribute to the rise in intracellular Ca^{2+}, and thus, muscle contraction (Liu *et al.* 2011).

1.4 RNAi Technology

RNAi technology is a useful research tool used to induce desired phenotypes without the need for genetic crosses. RNAi requires a double stranded RNA (dsRNA) that is cleaved to form a small interfering RNA (siRNA). Specific siRNAs can be designed to target specific genes. The delivered siRNA is incorporated into the RNA-induced silencing complex (RISC), where it induces specific degradation of the target mRNA. This inhibits effective translation of the mRNA, and the loss of translation leads to the desired phenotype (Kim and Rossi 2008). For *C. elegans*, dsRNA for corresponding genes can be expressed in *E. coli*, the primary bacterial food for *C. elegans*. This is done by inserting the coding region into a plasmid vector, that is transcribed from both strands upon activation of T7 promoters with IPTG. This is a

significantly effective way to induce RNA interference and an excellent tool to induce the phenotype in a large population of animals (Timmons and Fire 1998).

1.5 Calcium-ATPase Genes

In a genome wide RNAi screen for altered sensitivity to levamisole, Chaya *et al.* discovered that loss of the plasma membrane Ca^{2+}-ATPase (PMCA) MCA-3, caused paralysis to occur at a much slower rate (Chaya *et al*. 2021). Ca^{2+} is transported from the cytosol to the extracellular space through this ATPase in order to restore proper intracellular Ca^{2+} levels. Previously MCA-3 was shown to be required for clathrin-mediated endocytosis, and this defect can be reduced by lowering Ca^{2+} levels, which is consistent with this protein having a role in controlling intracellular Ca^{2+} (Bednarek *et al.* 2007).

MCA-3 uses active transport with ATP as an energy source to move the Ca^{2+} inside the cell, that becomes abundant during muscle contraction, to the extracellular space to aid in returning Ca^{2+} levels to homeostatic levels. In human cardiac muscle cells, homeostatic levels have intracellular Ca^{2+} levels at a concentration of 10^{-4} mM, extracellular concentration of 1mM, and sarcoplasmic reticulum concentration of 10^{-1} mM (Melkikh and Sutormina 2008). While similar Ca^{2+} levels have not been quantified in *C. elegans*, the relationship between these concentrations are the same, showing the importance of Ca^{2+}-ATPase restoration of homeostasis against the concentration gradient. MCA-3 knockdown has shown to be resistant to levamisole induced paralysis (Chaya *et al.* 2021). This was extremely surprising as it suggests that

intracellular Ca^{2+} levels are being reduced even more efficiently to result in resistance to levamisole-induced paralysis in the absence of MCA-3. This observation suggests that other mechanisms play an important role in restoring Ca^{2+} levels after muscle contraction.

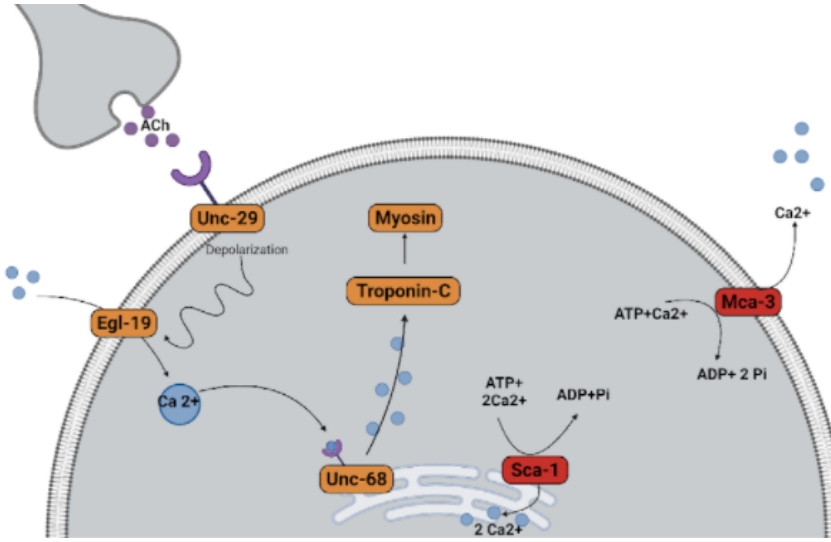

Figure 2: Roles of Ca^{2+}-ATPases

Intracellular calcium is reduced by Ca^{2+}-ATPases: SCA-1 and MCA-3.

The sarcoplasmic reticulum Ca^{2+}-ATPase (SERCA) SCA-1 brings two Ca^{2+} calcium back to the sarcoplasmic reticulum for every one ATP molecule, thus working together with MCA-3 to lower cytoplasmic Ca^{2+}. SCA-1 has also been shown to regulate the postsynaptic abundance of the levamisole-insensitive ionotropic AChR, ACR-16. Mutation of SCA-1 results in the mislocalization of ACR-16, causing decreased synaptic function and transmissibility (Martin and Richmond 2018). ACR-

16 is a vital protein, as receptors containing ACR-16 are responsible for all non-levamisole-sensitive synaptic signaling at the *C. elegans* NMJ (Touroutine *et al.* 2005*).* The effect of *sca-1* knockdown on levamisole-induced paralysis is currently unknown.

1.6 Objectives and Hypothesis

ATP availability plays a crucial role in levamisole-induced paralysis. When cellular ATP levels are low, Ca^{2+} cannot be pumped out of the cytoplasm at its normal pace, causing the muscles to remain contracted (Galimov *et al.* 2018). In an RNAi screen conducted in the Tanis lab, knockdowns of genes known to play a role in ATP synthesis were identified to cause levamisole hypersensitivity. This shows that reduced ATP synthesis increases sensitivity to levamisole, thus accelerating death (Chaya *et al.* 2021). MCA-3 only removes a single calcium ion from the cytoplasm per molecule of ATP. SCA-1, is much more efficient and is able to transport two calcium ions per ATP molecule used (Ingesi and De Meis 1989). I hypothesize that mutation of each gene individually will cause altered phenotype and paralysis rates due to the difference in ATP utilization.

The goal of my research was to investigate the effects of Ca^{2+} ATPase mutations on levamisole-induced paralysis rate as well as calcium levels in the postsynaptic body-wall muscles and ATP levels in the presence and absence of levamisole. The first aim was to determine effects of loss of *mca-3* and *sca-1* on levamisole induced

paralysis relative to the wild type control. The second aim was to evaluate ATP levels in animals with loss of *mca-3* and *sca-1* compared to the control both prior to and post levamisole exposure to determine if a difference in ATP levels could be connected to observed paralysis rates. My third aim was to study calcium levels through fluorescence microscopy using *C. elegans* expressing the Ca^{2+} indicator GCaMP, imaging animals before and after levamisole treatment.

Chapter 2

Methods

2.1 Nematode Maintenance

Nematode growth media (NGM) as described in (Brenner 1974) was used for animal growth and maintenance. NGM media was autoclaved for sterilization and set stirring at 70℃. Using a plate pouring pump, media was dispensed in the appropriate volume: 10 ml for 6 cm plates. After the agar fully set, plates were seeded with 200 µl of OP50 bacteria grown in B Broth. OP50, a uracil requiring mutant of *E. coli*, was used as the food source for standard animal maintenance. Since NGM lacks uracil, *E. coli* overgrowth can't occur, which makes it an ideal food source to ensure worm visibility (Brenner 1974). To maintain the *C. elegans*, 3-4 worms were picked using a platinum wire from an existing plate to a fresh plate. These plates were stored at either 15℃ or 20℃.

Table 1: *C. elegans* strains

Strain	**Gene/ Allele**	**Purpose**	**Media**	**Bacteria**	**Temperature**
N2 (Bristol)	wild type	Levamisole Assay	NGM	OP50	15℃ or 20℃
TR2171	*unc-68 (r1162)*V	Levamisole Assay	NGM	OP50	15℃ or 20℃

FX05339	*sca-1 (tm5339)* III	Levamisole Assay	NGM	OP50	15°C or 20°C
GS2526	*mca-3 (ar492)* IV	Levamisole Assay	NGM	OP50	15°C or 20°C
GR1373	*eri-1 (mg366)* IV	RNAi Levamisole Assay, ATP Assay	NGM, RNAi	OP50, RNAi clones	15°C or 20°C
MT1212	*egl-19 (n582)* IV	Levamisole Assay	NGM	OP50	15°C or 20°C
DA695	*egl-19 (ad695)* IV	Levamisole Assay	NGM	OP50	15°C or 20°C
AQ2953	*ljls131*[pmyo3::GCaMP3-SL2-tagRFP-T] IV	Calcium Imaging	NGM, RNAi	OP50, RNAi clone	15°C or 20°C
AQ2954	*ljls132*[pmyo-3::GFP-SL2-tagRFP-T]	Calcium Imaging	NGM, RNAi	OP50, RNAi clone	15°C or 20°C

2.2 RNAi

RNAi plates were made by adding 1 mL 1M Isopropyl β-D-1-thiogalactopyranoside (IPTG) and 1 mL Carbenicillin (25 mg/mL) per liter of NGM media. The addition of IPTG makes the media light sensitive, thus plates made for RNAi were wrapped in aluminum foil. RNAi media was dispensed in the same

amounts as NGM media: 20ml for 10 cm, 10ml for 6cm plates and 2 ml for 24 well plates.

To grow RNAi bacterial cultures, RNAi clones were streaked onto carbenicillin treated plates and grown overnight at 37℃. Then, a single colony was picked into a culture tube containing 3 ml of LB Broth with 3 µl of carbenicillin and left shaking overnight at 37℃. This culture was then used to seed RNAi plates. In an aseptic environment, 500 µl was transferred for 10cm plates, 200 µl was transferred to 6 cm plates, and 30 µl was seeded onto 24 well plates for each RNAi clone. The *sca-1* RNAi clone was diluted in a 3:1 fashion, with 1 ml of *sca-1* clone for every 3 ml of empty vector clone. As the *sca-1* null mutation is lethal, the dilution allowed for some knockdown of *sca-1* while still allowing *C. elegans* to fully complete their life cycle. *eri-1*(mg366) mutant *C. elegans* are RNAi hypersensitive. This strain was grown on RNAi plates in order to increase knockdown.

2.3 Levamisole Assay

The following protocol is from a paper, “Measuring *C. elegans* sensitivity to the acetylcholine receptor agonist levamisole”, currently under revision at JoVE, on which I am first author.

Part 1: Preparing Plates for the Levamisole Assay

1. Prepare nematode growth medium (NGM) media by combing 3 g NaCl, 2.5 g, BactoPeptone, and 17 g BactoAgar with 1 L of DI water in a flask with stir bar.
2. Autoclave, then put the media on a hot plate set to 70˚C and a stir at a moderate speed for one hour.
3. Add 1 ml of 5 mg/ml cholesterol dropwise to prevent precipitation, 1 ml of 1 M $CaCl_2$, 1 ml of 1 M $MgSO_4$, and 25 ml of 1 M pH 6.0 KH_2PO_4 to the media.
4. Transfer 2 ml of NGM media into each well of a 24 well plate with a sterile serological pipette (Figure 3).
5. Allow plates to dry on the benchtop for 2 days before seeding with bacteria; for longer term storage, place at 4˚C.
6. Streak out OP50 *E. coli* on a LB plate and grow overnight at 37°C.
7. Pick a single OP50 colony into B-broth (10 g tryptone, 5 g NaCl, 1 L DI H_2O) and set the culture shaking at 37°C overnight.
8. Using a sterile pipet drop 30 µl of OP50 suspension onto the agar in the middle of each well (Figure 3).

   NOTE: Be sure not to damage the agar surface as this will lead to worm burrowing.
9. Let the plates sit at least 2 days after seeding to allow a bacterial lawn to form.

   NOTE: Plates should be poured and seeded with bacteria the week before the assay. If bacteria in center wells is not dry after 2 days, leave plates open in hood for 20 minutes.

Part 2: Synchronizing *C. elegans* (DAY 1)

1. Grow *C. elegans* to adulthood on 6 cm plates, preparing at least 8 plates per strain

   NOTE: This is twice as many plates as needed, however, it is important to have back up plates in case the first batch of eggs are destroyed during bleach prep.
2. Prepare bleaching solution under the hood: mix 10 ml bleach, 2.5 ml 10 N NaOH, and 37.5 ml DI H_20 in a 50 ml conical tube.
3. Using a plastic transfer pipet, wash gravid adult worms from at least 4 plates with 1x M9 buffer and transfer into a 15 ml conical tube.
4. Spin down 1 min at 2000 rpm, then remove the supernatant using a transfer pipet
5. Add 10 ml of bleach solution, then invert / gently shake the tube ~4 minutes, until most of the worm carcasses have dissolved (Figure 3).

   NOTE: Be careful not to over-bleach the worms as this will destroy the eggs.
6. Spin down 1 min at 2000 rpm.
7. Pour off bleach solution in one motion; as long as the tube is not shaken at this point, the eggs will stick to the side of the tube.
8. Add 15 ml of M9 buffer and invert, spin down 1 min at 2000 rpm, and then pour off M9 buffer in one smooth motion.
9. Perform 3 total washes with M9 buffer as described in step 8.

10. After the final wash, add 10 ml fresh M9 and place on a rotator overnight at 15°C to isolate a synchronized population of starved first larval (L1) stage animals.

    NOTE: Before placing on rotator, check to make sure that there are eggs in the M9 buffer. If not, repeat the prep with back up plates and bleach for a shorter time.

Part 3: Plating Synchronized *C. elegans* (DAY 2)

1. Print out a 24-well plate map and assign strains to randomized places; each strain should be represented in the 24 well plate at least 6 times.
2. The day after performing the bleach prep, spin down worms at 2000 rpm for 1 min.
3. Remove ~ 9 ml of M9 with a plastic transfer pipet, then gently mix the starved first larval stage worms (L1s) in the remaining M9.
4. Immediately pipet 3 µl of the worms in M9 onto a microscope slide and determine the number of L1s; the desired number is 20-30 L1s in 3 µl. Spin down and remove M9 if the worm concentration is too low, add M9 if the concentration is too high.

    NOTE: Check the number of worms per 3 µl at least twice, inverting the tube each time.
5. Pipet 3 µl of L1s (20-30 worms total) into each well according to the pre-made plate map (Figure 3).

NOTE: Invert the tube with the L1s in M9 frequently to maintain an even distribution of worms as they will settle to the bottom. If this is not done, some wells will have too few worms, while others will have too many. Also, do not pierce the agar with the pipet tip as this will cause the animals to burrow.

6. Let the worms grow to adulthood, 3 days at 20°C.

   NOTE: Use of different growth temperatures and certain mutations can impact maturation speed so be sure to consider the *C. elegans* life cycle.

Part 4: Performing the Levamisole Assay (DAY 5)

1. Print a blank data sheet, which allows students to record the number of worms moving in each well every 5 minutes for one hour.

   NOTE: Students will be able to count worms in at most 12 wells every 5 minutes. One option is to have them work in pairs with the first student assaying the top 12 wells for one hour and the second student performing the assay in the subsequent hour. Alternatively, a plate with only 12 wells filled can be prepared for each student.

2. Check the worms in the 24 well plates. Using a sharpie, make an "X" on the plate lid over any wells that have contamination or too many worms (>40) , which will make counting difficult.

3. Make 0.4 mM levamisole solution by adding 200 µl of 100 mM levamisole to 50 mL M9

   NOTE: Levamisole must be diluted in M9; dilution in H_2O accelerates paralysis.

4. Start a timer, then using a transfer pipet, flood the first two wells with 0.4 mM levamisole such that the animals are freely swimming. Continue to add levamisole to adjacent wells, staggering the time according to the number of wells to be assayed.

   NOTE: For example, if 10 wells are assayed, levamisole will be added in the following manner: wells 1,2 at time 0, wells 3,4 after 1 minute, wells 5,6 after 2 minutes, wells 7,8 after 3 minutes, and wells 9,10 after 4 minutes.

5. At 5 minutes, start counting the number of moving worms in each well, starting with the first well, and record that number on the data sheet (Figure 3).
6. Continue to count the number of moving worms in each well every 5 minutes for an hour.

   NOTE: Students need to keep an eye on the timer as they will sometimes get behind during early time points before many worms paralyze. Depending on student experience level, it may be necessary to reduce the number of wells assayed.

7. When time permits, or at the end of the assay, record the total number of worms in each well.
8. Repeat steps 4-7 for the rest of the wells in the plate.

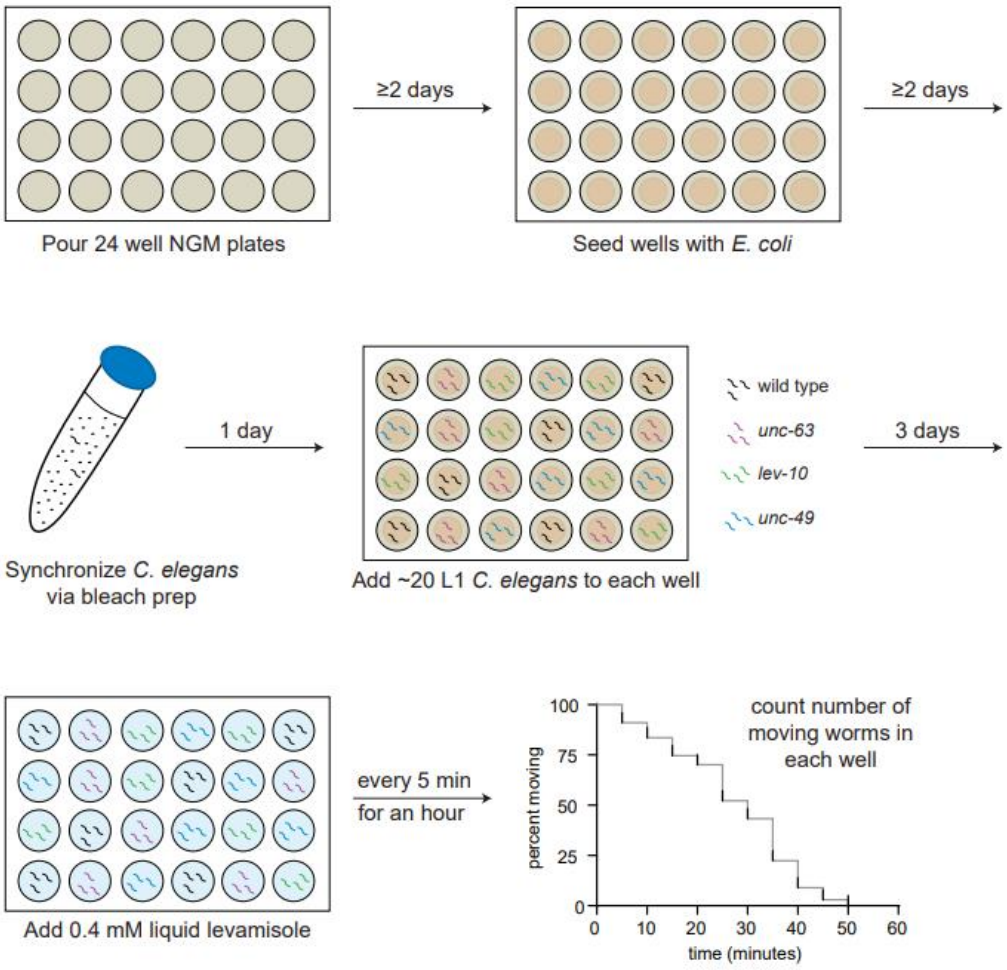

Figure 3: Levamisole Swim Assay Schematic

NGM plates were poured and seeded with *E. coli*. *C. elegans* were prepared via bleach prep and were added to previously prepared plates. After growth to adulthood, levamisole was added to the wells and moving animals were counted every 5 minutes.

Part 5: Data Analysis

1. Obtain the plate map for the assay (part 3, step 1), and record which strain corresponds to each well.
2. Enter data into an excel spreadsheet, organizing by genotype.
3. Combining data from wells, determine the number of worms moving at each time point for every strain.
4. Use these data to create a survival curve. Make a data table in either GraphPad Prism or Microsoft Excel; the left hand column should indicate time and subsequent columns contain data for each strain. For each animal that paralyzed within the first 5 minutes, create a row and enter a "1" for 5 minutes; do this for each time point. For all animals that do not paralyze by the end of the assay, enter a "0" at 60 minutes. Pairwise comparisons using the log-rank (Mantel Cox) test should be performed to determine if there is statistical significance between two different strains.

NOTE: Due to the amount of data collected, this analysis and subsequent discussion of the data will take at least a couple of hours

2.4 ATP Quantification Assay

ATP quantification assays were performed with the ATP Bioluminescence Assay Kit CLS II (Roche Diagnostics) as described (Chaya *et. al* 2021) with modifications. Since RNAi was used, *eri-1* worms were bleached and spotted onto 10 cm plates, about 1000 worms per plate. Three plates were made for each RNAi clone of interest*:*

sca-1, mca-3, and EV. One plate of each strain was exposed to the following conditions: 0 min in 0.4 mM levamisole, 30 min in 0.4 mM levamisole, and 60 min in 0.4 mM levamisole. *C. elegans* were washed 3 times with 1x M9 solution and 20 µL of worms were transferred to microcentrifuge tubes. 180 µL of boiling Tris-EDTA buffer (100 mM Tris, 4 mM EDTA pH 7.75) was added and samples were incubated at 100 °C for 2 minutes, sonicated for 3 minutes and then centrifuged at 14,000 RPM for 10 minutes at 4 °C. 40 µL of the supernatant was added to 360 µL Tris-EDTA buffer to make 1:10 dilutions for triplicate technical replicates. ATP content was determined following the Roche ATP Bioluminescence Assay Kit CLS II protocol using a Glomax 96 Microplate Luminometer. ATP levels were normalized to total protein content using the Pierce BCA protein assay kit (Chaya *et al.* 2021)

2.5 *C. elegans* Calcium Imaging

AQ2954 and AQ2953 animals were grown on RNAi plates as described above in order to achieve knockdown while maintaining detectable fluorescence. For imaging, an agarose pad was made by placing a drop of melted 3% agarose on a microscope slide. Another microscope slide was immediately placed directly on top. After about a minute, the microscope slides were pulled apart to reveal the agarose pad. 3 µl of 0.1µm diameter polystyrene microsphere solution was added to the center of the agar pad. Use of a microsphere solution allowed for worms to be immobilized for imaging without the need of a paralytic. *C. elegans* were quickly picked into the microsphere

solution. After approximately 3 worms were placed into the solution, a coverslip was placed on top before imaging.

Imaging was conducted on a Zeiss LSM880 confocal microscope. Images were taken with a 20x objective. tagRFP in the muscles was imaged along with green fluorescence GCaMP3 in each capture. GCaMP3 is a calcium indicator made of (GFP), calmodulin and the M13 domain of a myosin light chain kinase. Florescence intensity is directly related to calcium availability, as calcium binding creates GFP fluorescence (Tian *et al.* 2009). The tagRFP expressed in the muscles along with the GCaMP3 is insensitive to changes in Ca^{2+} concentration and thus can be used for normalization. Separate paths were used to excite both red and green fluorescent proteins.

2.6 Statistical Analysis

For levamisole swim assays, pairwise comparisons using the log-rank (Mantel Cox) test (GraphPad Prism) were performed to determine if there is statistical significance between two different strains.

Chapter 3

Results

3.1 Time- Dependent Levamisole Induced Paralysis in Mutant *C. elegans*

Levamisole selectively binds to L-AChRs on the body-wall muscles of *C. elegans*. Levamisole binding causes muscle hypercontraction leading to time dependent paralysis and death of the animal (Martin *et al.* 2012). Various mutants were studied through levamisole swim assays to determine the differences in time dependent paralysis. *unc*-68 and *egl*-19 mutations were used as controls for comparison, as their role in levamisole induced paralysis is already known. UNC-68 is found on the sarcoplasmic reticulum and binding of Ca^{2+} to this ryanodine receptor releases Ca^{2+} from stores in the sarcoplasmic reticulum into the intracellular space. EGL-19 is a voltage gated Ca^{2+} channel that brings Ca^{2+} into the intracellular space (Liu *et al.* 2011). MCA-3, a PMCA, reduces intracellular Ca^{2+} to return cells to homeostasis after muscle contraction. MCA-3 was identified in a previous RNAi screen as having a levamisole resistant phenotype (Chaya *et al.* 2021). The SERCA SCA-1 works in concert with MCA-3 to reduce intracellular Ca^{2+} by returning the Ca^{2+} to the sarcoplasmic reticulum, and its levamisole phenotype is currently unknown.

Sixty-minute levamisole swim assays were conducted to determine how post-synaptic mutations in Ca^{2+} ATPases affect time-dependent paralysis. 0.4 mM levamisole results in paralysis ($p<0.0001$) compared to swimming in M9 alone (Figure 4). *unc-68* mutants paralyzed significantly slower ($p<0.05$) slower compared to control

wild type worms (Figure 5). This suggests that *unc-68* has a resistant phenotype, as its normal function to increase Ca^{2+} levels helps to induce paralysis. *mca-3* mutants paralyzed significantly slower ($p<0.0001$) compared to wild type, suggesting a levamisole resistant phenotype (Figure 6). This phenotype matches published research (Chaya *et al*., 2021). Loss of *sca-1* resulted in a hypersensitive phenotype, as the mutants paralyzed significantly faster ($p<0.0001$) than wild type (Figure 7). This suggests that SCA-1 plays a key role in reducing intracellular Ca^{2+} upon muscle contraction, as without it, Ca^{2+} build up, which leads to paralysis, occurs much faster. *egl-19* gain of function animals paralyzed significantly faster ($p<0.0001$) than wild type, indicating a hypersensitive phenotype (Figure 8). However, paralysis of *egl-19* loss of function mutants was not significantly different from wild type ($p=0.3485$). This indicates that additional calcium influx by EGL-19 can speed paralysis, but elimination does not affect paralysis rate, suggesting other mechanisms of Ca^{2+} influx play a significant role.

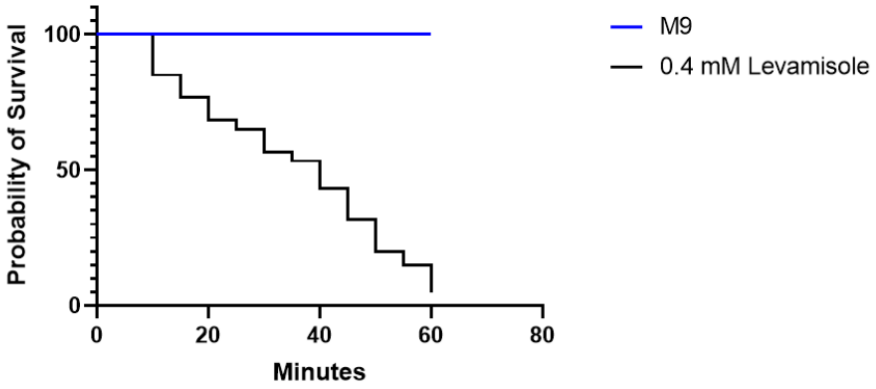

Figure 4: Levamisole Induces Time-Dependent Paralysis

Treatment with 0.4 mM levamisole (black) caused significant paralysis ($p<0.0001$) compared to 1xM9 buffer (blue)

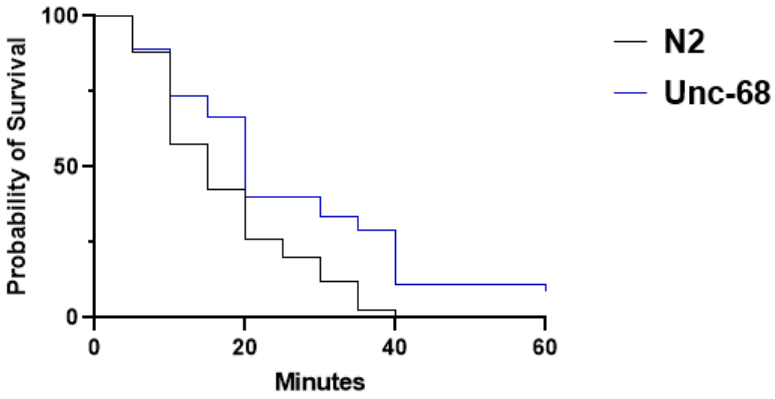

Figure 5: Mutation of *unc-68* Causes Levamisole Resistance

unc-68 mutants (blue) paralyzed significantly slower ($p<0.05$) than wild type N2 (black) after treatment with 0.4 mM levamisole, indicating levamisole resistance

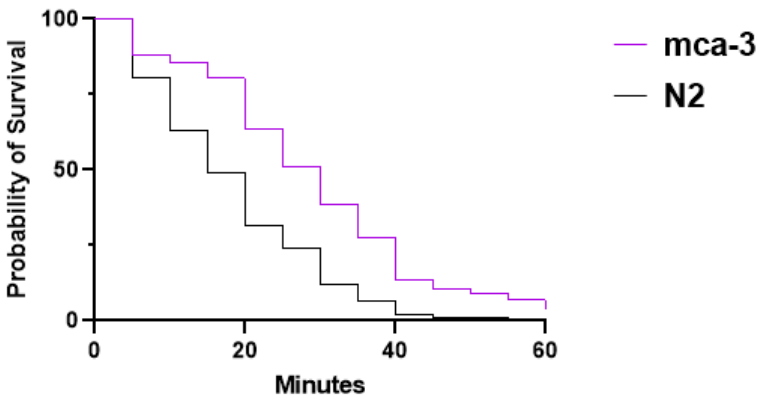

Figure 6: Mutation of *mca-3* Causes Levamisole Resistance

mca-3 mutants (pink) paralyzed significantly slower ($p<0.0001$) than wild type N2 (black) after treatment with 0.4 mM levamisole, indicating levamisole resistance

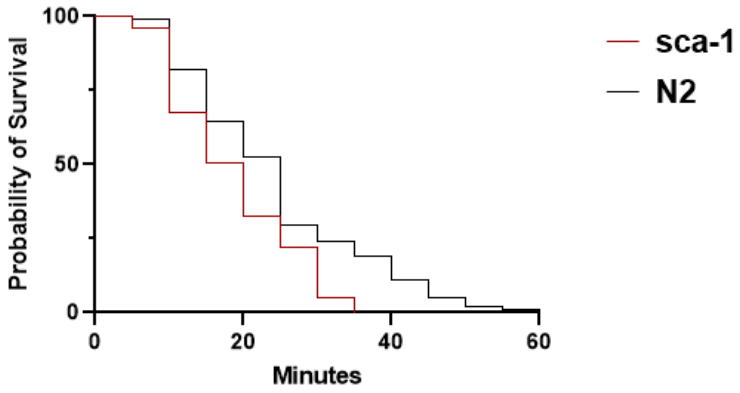

Figure 7: Mutation of *sca-1* Causes Levamisole Hypersensitivity

sca-1 mutants (red) paralyzed significantly faster ($p<0.0001$) than wild type N2 (black) after treatment with 0.4 mM levamisole, indicating levamisole hypersensitivity.

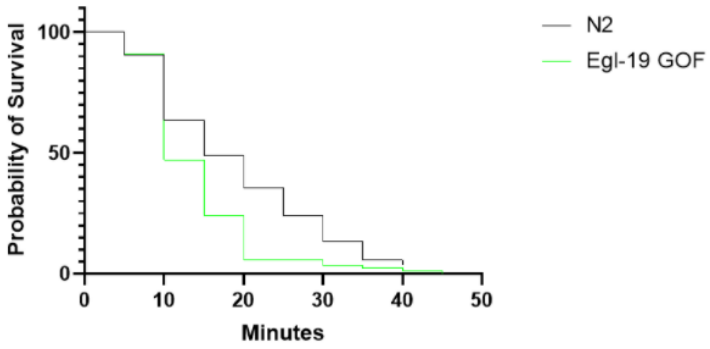

Figure 8: Gain of Function Mutation of *egl-19* Causes Levamisole Hypersensitivity

Mutation of *egl-19* (green) paralyzed significantly slower (p=<0.0001) than N2 (black) after treatment with 0.4 mM levamisole ,indicating levamisole hypersensitivity.

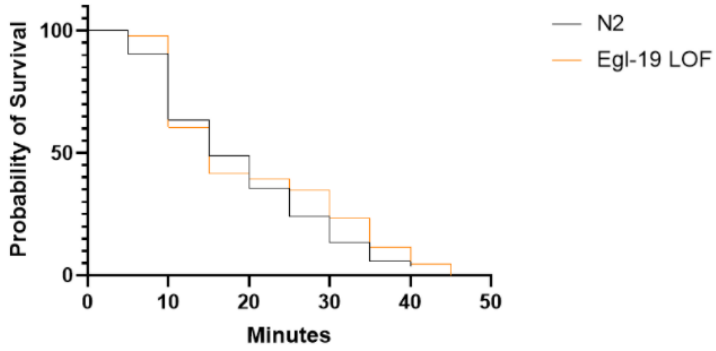

Figure 9: Loss of Function Mutation of *egl-19* Causes Insignificant Levamisole Paralysis

Loss of function mutation of *egl-19* (orange) did not paralyze at a significantly different rate (p= 0.3485) compared to N2 (black) after treatment with 0.4 mM levamisole

3.2 Time -Dependent Levamisole Induced Paralysis in RNAi knockdown *C. elegans*

RNAi knockdown is an extremely useful research tool to induce loss of function phenotypes. One method of RNAi technology in *C. elegans* involves feeding animals *E. coli* containing dsRNA. This dsRNA results in the targeting of transcripts from desired genes and prevents translation, resulting in a mutant phenotype (Kim and Rossi 2008). In my case, RNAi knockdown was used to determine if the levamisole induced paralysis phenotypes found using RNAi technology matched those of mutant animals, so that RNAi could be utilized in future experiments.

unc-68 RNAi caused significantly slower paralysis ($p<0.0001$) compared to empty vector (Figure 10). This matches the data collected from mutant animals, where the *unc-68* mutation caused levamisole resistance (Figure 5). *mca-3* RNAi also caused significantly slower paralysis ($p<0.0001$) than the empty vector (Figure 11), showing a levamisole resistant phenotype. This also matches data collected with *mca-3* mutant *C. elegans* (Figure 6). Finally, *sca-1* RNAi caused faster paralysis ($p<0.0001$) than the empty vector (Figure 12). This hypersensitive phenotype matches *sca-1* mutant assays (Figure 7).

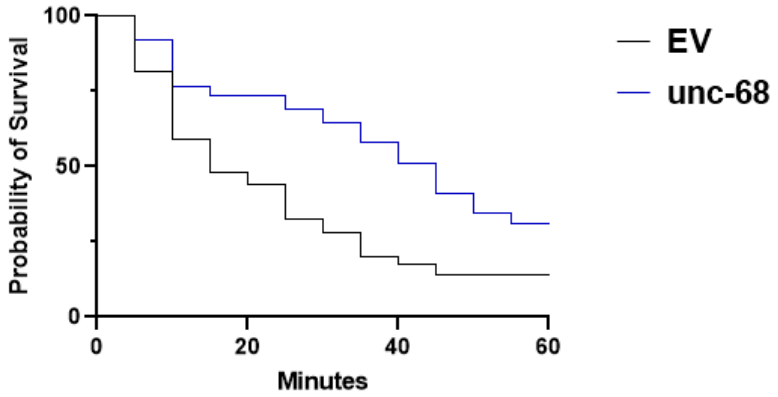

Figure 10: *unc-68* RNAi Knockdown Results in Levamisole Resistance

RNAi knockdown of *unc-68* (blue) caused significantly slower paralysis compared to the EV control (black) indicating levamisole resistance ($p<0.0001$).

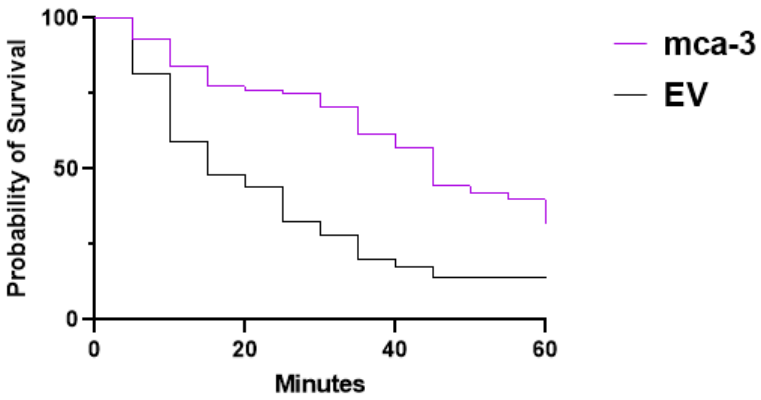

Figure 11: *mca-3* RNAi Knockdown Results in Levamisole Resistance

RNAi knockdown of *mca-3* (pink) caused significantly slower paralysis compared to the EV control (black) indicating levamisole resistance ($p<0.0001$).

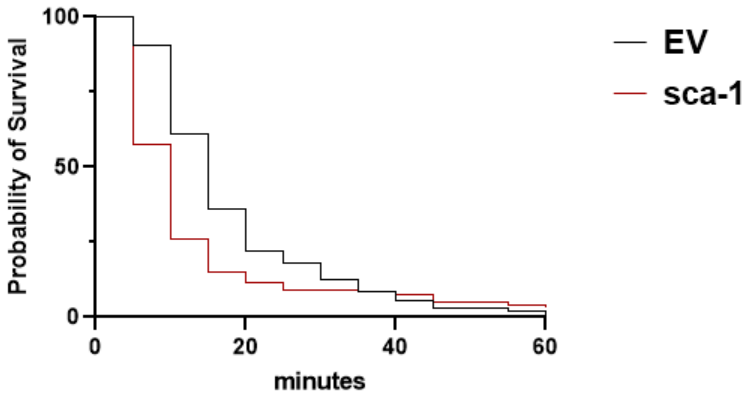

Figure 12: *sca-1* RNAi Knockdown Results In Levamisole Hypersensitivity

RNAi knockdown of *sca-1* (red) caused significantly faster paralysis compared to the EV control (black) indicating levamisole hypersensitivity ($p<0.0001$).

3.3 ATP Quantification

ATP is a vital molecule in all living organisms as a major source of energy. Ca^{2+}ATPases, such as MCA-3 and SCA-1 use ATP to reduce intracellular Ca^{2+} after muscle contraction. Levamisole-induced depletion of ATP or buildup of Ca^{2+} can lead to total paralysis and eventual death. ATP quantification can reveal if changes in available ATP could be a contributing factor to the paralysis trends observed with the Ca^{2+}ATPase mutants. I observed that loss of *sca-1* mutation caused hypersensitivity to levamisole (Figure 7,12), while loss of *mca-3* mutation resulted in resistance (Figure 6,11). For ATP quantification, *eri-1(mg366)* animals were fed *E. coli* with *sca-1*, *mca-3* or EV RNAi clones. ATP levels were calculated using measured luciferase

luminesce and normalized to protein concentration. ATP was quantified after 0, 30 and 60 minutes of 0.4mM levamisole treatment. These times were selected to detect changes in ATP before, during, and after paralysis.

Treatment with 0.4 mM levamisole showed significant decreases of ATP levels over 60 minutes, however the rate at which this ATP depletion occurs varied among the different knockdowns used. Empty vector (EV) RNAi was utilized as a control. EV resulted in significant ATP depletion over the course of the entire 60 minutes of treatment ($p<0.0001$), though no significant change in ATP during the first 30 minutes ($p=0.5875$) or between 30 and 60 minutes of treatment ($p=0.2572$) was observed (Figure 13). *sca-1* knockdown resulted in significant ATP depletion ($p=0.0153$) over the first 30 minutes of 0.4 mM levamisole treatment, but no significant change ($p=0.1168$) between 30 and 60 minutes of treatment (Figure 14). This suggests that most of the levamisole induced ATP depletion occurs quickly in *sca-1* knockdown animals, with the only significant change occurring in the first 30 minutes. However, *mca-3* showed no significant decrease ($p=0.3081$) over the first 30 minutes of treatment, but saw a significant decrease ($p=0.0062$) over the last 30 minutes of treatment (Figure 15). This is different from the trends seem in *sca-1* knockdown, as significant ATP depletion did not occur until the last thirty minutes of levamisole treatment.

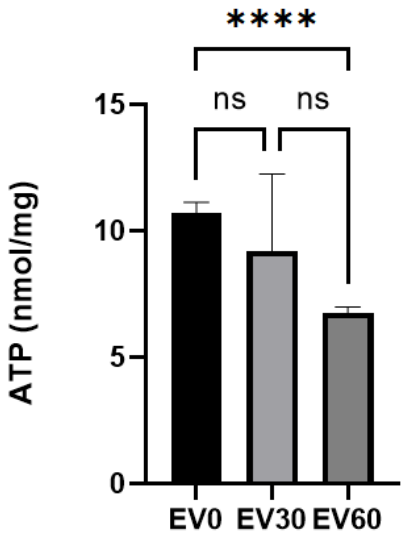

Figure 13: Levamisole Exposure Causes Significant ATP Depletion Over Sixty Minutes

In animals fed EV *E. coli* with no gene knockdown ATP levels were significantly lower ($p<0.0001$) between 0 and 60 minutes of 0.4mM levamisole treatment. There was no significant depletion between 0 and 30 minutes ($p=0.5875$) and 30 and 60 minutes of treatment ($p=0.2572$).

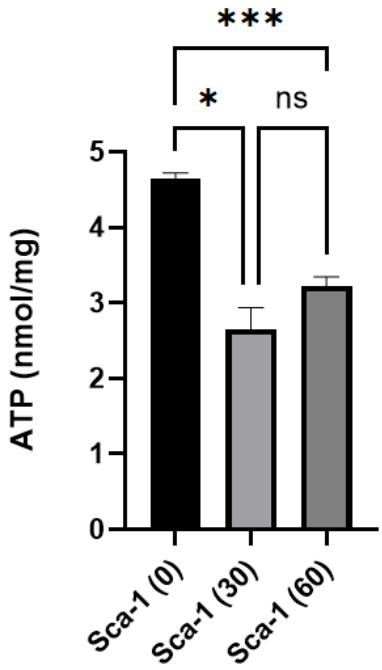

Figure 14: *sca-1* Knockdown Causes Significant ATP Depletion Within Thirty Minutes of Levamisole Exposure

Following *sca-1* knockdown, ATP levels were significantly lower (p=0.0153) between 0 and 30 minutes of 0.4mM levamisole treatment, and significantly slower over the course of 60 minutes (p=0.0010). There was no significant depletion between 30 and 60 minutes of treatment (p=0.1168).

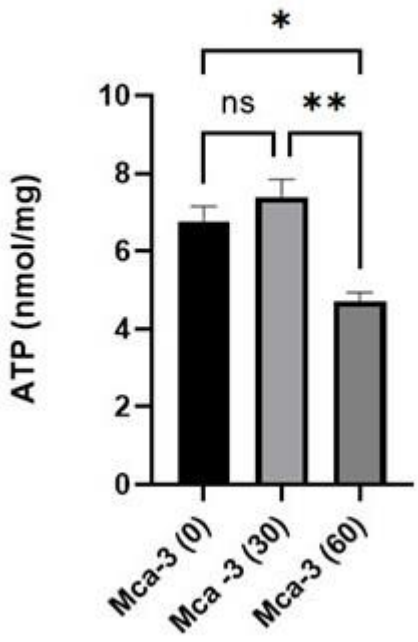

Figure 15: *mca-3* Knockdown Results in ATP Depletion Over Sixty Minutes of Levamisole Exposure

Knockdown of *mca-3* resulted in no significant ATP depletion ($p= 0.3081$) over the first 30 minutes of 0.4mM levamisole treatment, and significant ATP depletion ($p<0.01$) over 60 minutes. ATP significantly decreased ($p<0.01$) between 30 and 60 minutes of levamisole treatment.

3.4 Florescence Calcium imaging

Intracellular Ca^{2+} build-up is a known cause for muscle paralysis. Florescence confocal imaging was conducted to visualize the change in intracellular Ca^{2+} before and after levamisole exposure. The strain AQ2953 (see table 1) contained GCaMP and tagRFP labelling, allowing calcium to be specifically marked for florescence. Since tagRFP is not sensitive to changes in Ca^{2+} levels, it serves as an internal control to ensure that confounding variables such as levamisole or RNAi technology were not dulling overall florescence. RFP florescence should not change over time, as muscle presence should not change. GCaMP3 is a calcium indicator made of (GFP), calmodulin and the M13 domain of a myosin light chain kinase. Ca^{2+} binds to this indicator creating a confirmational change, resulting in GFP florescence. GFP florescence intensity is directly proportional to Ca^{2+} availability (Tian *et al.* 2009). *C. elegans* were grown on RNAi plates containing empty vector *E. coli*. Surveying florescence intensity over the duration of levamisole treatment could give insight to the relationship between Ca^{2+} availability and muscle contraction. Florescence imaging was conducted after 0 minutes, 10 minutes, and 60 minutes of 0.4 mM levamisole treatment. Figure 16 represents optimized imaging parameters that can easily be applied to future image collection. Qualitatively, a change in GFP fluorescence does not seem to appear over the course of 60 minutes, however, quantitative analysis of a larger sample size is needed to confirm.

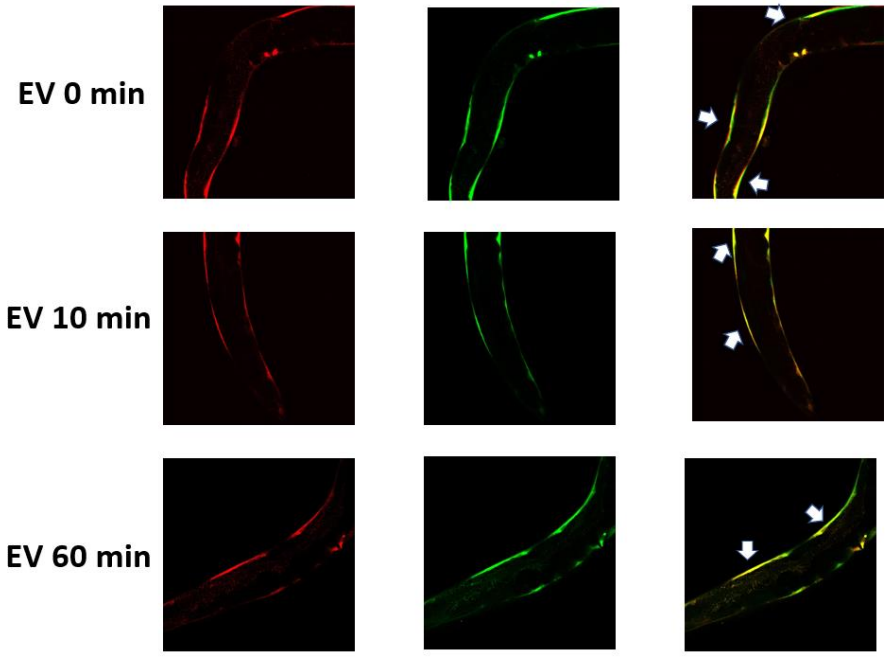

Figure 16: Representative Images of GCaMP Fluorescence after EV Insertion

Representative images of tagRFP (left) and GCaMP3 (middle) fluorescence over the course of 60 minutes of 0.4 mM levamisole treatment; merge (right)Arrows indicate muscles of interest.

Chapter 4

Discussion

While previous genomic screens have identified muscle-expressed genes responsible for levamisole signaling and subsequent induced paralysis, little was known about why loss of the PMCA MCA-3 caused a levamisole resistant phenotype. Further, the SERCA SCA-1 had not been investigated for its levamisole phenotype and role in working in concert with MCA-3. The purpose of this study was to investigate the molecular cause of significantly different levamisole induced paralysis rates in the PMCA and SERCA mutants, including levels of ATP and differences in intracellular Ca^{2+} availability. Understanding the roles of MCA-3 and SCA-1 will allow greater insight into the impact of these Ca^{2+}ATPases on intracellular Ca^{2+} and ATP and homologous proteins could affect neuromuscular function in humans.

Body wall muscles of *C. elegans* are functionally equivalent to the skeletal muscles of humans, making them an excellent model organism to study the NMJ (Gieseler 2017). Sensitivity to levamisole, an AChR agonist, was used to determine how paralysis rates varied among several mutant strains. *unc-68* mutation and RNAi knockdown caused a levamisole resistant phenotype. UNC-68 is responsible for releasing Ca^{2+} stores from the sarcoplasmic reticulum into the intracellular space, to further increase calcium build up for full muscle contraction and eventual paralysis (Liu *et al*. 2011). In this UNC-68 mutant, the receptor is rendered useless and unable to bind with Ca^{2+} to release Ca^{2+} from the sarcoplasmic reticulum. Without release of Ca^{2+} from the sarcoplasmic reticulum, Ca^{2+}ATPases can maintain intracellular Ca^{2+}

levels for a longer period of time to withhold paralysis, creating the observed resistant phenotype.

A gain of function mutation in *egl*-19, which allows for constitutive Ca^{2+} influx, resulted in faster intracellular Ca^{2+} build up and thus faster paralysis in response to levamisole (Liu *et al.* 2011). However, the loss of function mutation of *egl-19* resulted in no significant difference in paralysis compared to wild type. These results indicate that EGL-19 plays an important role in Ca^{2+} entry, but other mechanisms of calcium influx can compensate to induce paralysis at the same rate when *egl-19* is eliminated. *egl-19* RNAi knockdown was not explored as RNAi clones could not be confirmed through DNA sequencing.

mca-3 mutation and RNAi knockdown both resulted in a levamisole resistant phenotype, with the animals paralyzing significantly slower than the wild type control. However, the mechanism behind this is unusual. MCA-3 works to reduce intracellular Ca^{2+}, so without it, it would be predicted that Ca^{2+} in the intracellular space would accumulate faster, leading to faster paralysis. However, the opposite phenotype is observed, suggesting there is another mechanism contributing to reducing intracellular Ca^{2+}. With *mca*-3 mutation, the cells are more efficiently preventing paralysis and thus reducing intracellular Ca^{2+} even though the PMCA mechanism of reducing this Ca^{2+} has been eliminated.

sca-1 mutation and RNAi knockdown resulted in a faster paralysis compared to the wild type control, indicating a levamisole sensitive phenotype. SCA-1 works to reduce intracellular Ca^{2+} levels by efficiently moving Ca^{2+} back into the sarcoplasmic

reticulum after muscle contraction. With a mutation of this gene, the cells are unable to restore low intracellular Ca^{2+} in the intracellular space, and the buildup of Ca^{2+} causes paralysis occurs much quicker. Since it is known that SCA-1 is more efficient than MCA-3, with SCA-1 moving 2 Ca^{2+}per ATP molecule, it is plausible that the mechanism contributing to MCA-3 levamisole resistance is the ability for SCA-1 to work alone. With an MCA-3 mutation, SCA-1 can use all of the ATP available in the cell to move Ca^{2+} at this more efficient rate, rather than having to compete with the less efficient MCA-3 for ATP to drive Ca^{2+} movement.

Levamisole assays are a simple, efficient way to study the NMJ in C. elegans. However, the assay does require proper preparation. First, bacterial lawns must be completely dry before spotting L1 animals into the wells. If not dried enough, the bacteria mixes with the levamisole solution during the assay, turning the liquid cloudy and preventing students from being able to count the worms. Second, when synchronizing worms through bleach prep, the animals must not be exposed to the bleach solution for too long as this will cause the protective coating on the eggs to disintegrate. Third, it is crucial to spot only 20-30 L1s per well, as too many worms in the wells makes it extremely difficult to accurately count the number moving in the time allotted. Finally, it is important to maintain aseptic technique during preparation of the plates as contaminated wells cannot be assayed.

Following confirmed time-dependent levamisole-induced paralysis, ATP levels were quantified. Previous literature has shown that treatment of control animals with

levamisole over sixty minutes reduces ATP significantly over time (Chaya *et al.* 2021). Examining the loss of ATP levels over time in mutant *C. elegans* could give insight into whether bioenergetic differences cause the paralysis phenotypes observed. Among EV, *sca-1*, and *mca-3* RNAi knockdown, all experienced significant decrease in paralysis over 60 minutes, however the speed at which this depletion occurred varied.

Animals fed the EV *E. coli* exhibited a significant decrease in ATP only over the course of the entire 60 minute 0.4 mM levamisole treatment, and no significant decrease during the first or second half of the treatment (Figure 13). This indicates that ATP depletion occurred slowly over the course of the sixty minutes, with significance only seen after the complete hour. However, the data only represents two biological replicates, so more experimentation is needed to confirm the described trends. The limited replicates created a high standard deviation (SD=3.967) at 30 minutes of levamisole treatment, which could impact the conclusions.

sca-1 knockdown resulted in a significant decrease in ATP over the first 30 minutes, and this level of depletion sustained over the last 30 minutes of levamisole treatment (Figure 14). As *sca-1* knockdown showed a levamisole hypersensitive phenotype, the quick depletion of ATP matches the quick levamisole-induced paralysis observed with loss of *sca-1*. As the mutant animals paralyze quickly, most reach complete paralysis and eventual death by 30 minutes, meaning that there is almost no metabolic function. Since the majority of the *C. elegans* are completely paralyzed after 30 minutes, there is not significant change in the ATP levels in the last 30 minutes of

levamisole treatment. However, Figure 14 represents technical replicates only, so more biological replicates are required to conclude complete trends.

mca-3 knockdown resulted in a significant decrease in ATP only between 30 and 60 minutes of levamisole treatment (Figure 15). Since *mca-3* showed a levamisole resistant phenotype, the slow depletion of ATP matches the slow paralysis rate of *mca-3.* Since the majority of mutant *C. elegans* have not yet reached paralysis within the first 30 minutes of levamisole treatment, there is still ATP available to prevent paralysis. However, the majority of *mca-3* knockdown animals are paralyzed by 60 minutes, which is consistent with the drop in ATP levels between 30 and 60 minutes. However, Figure 15 represents technical replicates only, so more biological replicates are needed.

Overall, the ATP assays present interesting trends, but more replicates are needed to confirm the data presented here. ATP assays require a Glomax 96 Microplate Luminometer with injection system to measure fluoresce from luciferase injection. However, the plate reader available in Wolf Hall, University of Delaware, had several malfunctions throughout the course of my research. These malfunctions resulted in some assays having to be redone or lost due to inconsistent injection by the plate reader. Additionally, the assay is extremely long, usually occurring over a few days. This leaves much room for error. These limitations obligated me to use technical replicates for s*ca-1* and *mca-3* knockdown, and further investigation is needed to confirm the trends described.

Ca^{2+} is known to be a key ion responsible for muscle contraction. Hence, I explored Ca^{2+} levels with GCaMP fluorescence imaging to investigate if a change in fluorescence intensity could be seen through various stages of paralysis. I was able to develop a microsphere method to prepare the animals for imaging that did not require paralytic, which could disrupt intracellular Ca^{2+} and ATP. First, imaging was conducted on a Zeiss Axio Zoom microscope, however the microscope was not sensitive enough for reliable imaging. The Zeiss LSM880 confocal microscope allowed for the elimination of bleed through and higher sensitivity, even at the 20x magnification used in these images. Ample time was spent perfecting laser and camera settings for optimal image collection. The representative images (Figure 16) show promise in the reliability of the imaging at three different time points, however a larger sample size is needed to conduct fluorescence intensity and statistical analysis. Future directions include imaging of animals with *sca-1* and *mca-3* knockdown to determine if there is a change of fluorescence intensity over the course of levamisole treatment.

Preparation of *C. elegans* for this imaging came with several limitations. First, transfer of paralyzed *C. elegans* from the 0.4 mM levamisole solution to the microscope slide was difficult. Animals were scooped from the liquid onto the agarose pad using a worm pick, requiring advanced precision given the size of the animals and surface tension of the liquid solution. This difficult transfer also had to be conducted quickly, as the time the *C. elegans* remained in the levamisole was a crucial aspect of the experiment. Additionally, microspheres were used to mount the worms for imaging.

These microspheres require that very little *E. coli* from the original maintenance plate be transferred onto the microspheres, as this can render them useless. This proved difficult for *C. elegans* imaged prior to levamisole treatment, or at 0 minutes. These animals had not been washed with the levamisole solution, and thus were transferred directly from maintenance plates. This transfer of minimal *E. coli* did not immobilize some animals, making them unable to be imaged with multiple channels. Finally, the Zeiss LSM 880 microscope malfunctioned multiple times during the Spring 2022 semester, delaying image collection.

In conclusion, this thesis looked to examine the impact of Ca^{2+} ATPases on levamisole induced paralysis and its molecular causes. SCA-1 deletion showed levamisole hypersensitivity, while MCA-3 deletion showed levamisole resistance. This suggests the increased efficiency of SCA-1 plays a key role in controlling intracellular Ca^{2+} levels after muscle contraction. *sca-1* knockdown showed significant decrease in ATP levels quickly, within the first 30 minutes of levamisole treatment. However, ATP levels depleted slower in *mca-3* knockdown, within the last 30 minutes of levamisole treatment. This matches the speed of paralysis seen in levamisole assays. Finally, representative imaging of GCaMP fluorescence imaging shows promise for future analysis and a way to investigate intracellular Ca^{2+} in the Ca^{2+} ATPase knockdowns. Overall, Ca^{2+} ATPases play a fundamental role in regulating intracellular Ca^{2+} levels and further investigation of the data presented in this thesis could provide continued clarity on how constant activity of these pumps could lead to bioenergetic failure.

REFERENCES

Bednarek E. M., L. Schaheen, J. Gaubatz, E. M. Jorgensen, and H. Fares, 2007 The plasma membrane calcium ATPase MCA-3 is required for clathrin-mediated endocytosis in scavenger cells of Caenorhabditis elegans. Traffic 8: 543–553. https://doi.org/10.1111/j.1600-0854.2007.00547.x

Brenner S., 1974 *THE GENETICS OF CAENORHABDITIS ELEGANS*.

Brown L. A., A. K. Jones, S. D. Buckingham, C. J. Mee, and D. B. Sattelle, 2006 Contributions from Caenorhabditis elegans functional genetics to antiparasitic drug target identification and validation: Nicotinic acetylcholine receptors, a case study. International Journal for Parasitology 36. https://doi.org/10.1016/j.ijpara.2006.01.016

Chaya T., S. Patel, E. M. Smith, A. Lam, E. N. Miller, *et al.*, 2021 A C. elegans genome-wide RNAi screen for altered levamisole sensitivity identifies genes required for muscle function. G3 Genes|Genomes|Genetics. https://doi.org/10.1093/g3journal/jkab047

Clapham D. E., 2007 Calcium Signaling. Cell 131 https://doi.org/10.1016/j.cell.2007.11.028

Corsi A. K., B. Wightman, and M. Chalfie, 2015 A Transparent Window into Biology: A Primer on *Caenorhabditis elegans*. Genetics 200. https://doi.org/10.1534/genetics.115.176099

Fleming, J. T., Squire, M. D., Barnes, T. M., Tornoe, C., Matsuda, K., Ahnn, J., Fire, A., Sulston, J. E., Barnard, E. A., Sattelle, D. B., & Lewis, J. A. (1997). Caenorhabditis elegans levamisole resistance genes lev-1, unc-29, and unc-38 encode functional nicotinic acetylcholine receptor subunits. *The Journal of neuroscience : the official*

journal of the Society for Neuroscience, *17*(15), 5843–5857. https://doi.org/10.1523/JNEUROSCI.17-15-05843.1997

Galimov E. R., R. E. Pryor, S. E. Poole, A. Benedetto, Z. Pincus, *et al.*, 2018 Coupling of Rigor Mortis and Intestinal Necrosis during C. elegans Organismal Death. Cell Reports 22. https://doi.org/10.1016/j.celrep.2018.02.050

Gieseler, K. Development, structure, and maintenance of C. elegans body wall muscle. *WormBook* 1–59 (2017) doi:10.1895/wormbook.1.81.2.Gally C., S. Eimer, J. E. Richmond, and J. L. Bessereau, 2004 A transmembrane protein required for acetylcholine receptor clustering in Caenorhabditis elegans. Nature 431: 578–582. https://doi.org/10.1038/nature02893

Inesi G, De Meis L. 1989. Regulation of steady state filling in sarcoplasmic reticulum. Roles of back-inhibition, leakage, and slippage of the calcium pump. J. Biol. Chem. 264:5929–5936.

Kim D. H., and J. J. Rossi, 2008 RNAi mechanisms and applications. BioTechniques 44. https://doi.org/10.2144/000112792

Liu P , Ge Q , Chen B , Salkoff L , Kotlikoff MI , et al. 2011. Genetic dissection of ion currents underlying all-or-none action potentials in C. elegans body-wall muscle cells. J. Physiol. 589:101–117.

Lewis J. A., C.-H. Wu, H. Berg, and J. H. Levine, 1980 *THE GENETICS OF LEVAMISOLE RESISTANCE IN THE NEMATODE CAENORHABDITIS ELEGANS*.

Martin, A. A., & Richmond, J. E. (2018). The sarco(endo)plasmic reticulum calcium ATPase SCA-1 regulates the Caenorhabditis elegans nicotinic acetylcholine receptor ACR-16. *Cell calcium*, *72*, 104–115. https://doi.org/10.1016/j.ceca.2018.02.005

Martin, R. J., Robertson, A. P., Buxton, S. K., Beech, R. N., Charvet, C. L., & Neveu, C. (2012). Levamisole receptors: a second awakening. *Trends in parasitology*, *28*(7), 289–296. https://doi.org/10.1016/j.pt.2012.04.003

Melkikh, Alexey & Sutormina, Maria. (2008). Model of active transport of ions in cardiac cell. Journal of theoretical biology. 252. 247-54. 10.1016/j.jtbi.2008.02.006.

Rand, J.B. Acetylcholine (January 30, 2007), *WormBook*, ed. The *C. elegans* Research Community, WormBook, doi/10.1895/wormbook.1.131.1, http://www.wormbook.org.

Richmond, J. E., & Jorgensen, E. M. (1999). One GABA and Two acetylcholine receptors function at the C. elegans neuromuscular junction. *Nature Neuroscience*, *2*(9), 791-797. doi:10.1038/12160

Riddle DL, Blumenthal T, Meyer BJ, et al., editors. C. elegans II. 2nd edition. Cold Spring Harbor (NY): Cold Spring Harbor Laboratory Press; 1997. Section II, Sexual Dimorphism. Available from: https://www.ncbi.nlm.nih.gov/books/NBK20094/

Robertson A. P., C. L. Clark, and R. J. Martin, 2010 Levamisole and ryanodine receptors (I): A contraction study in Ascaris suum. Molecular and Biochemical Parasitology 171. https://doi.org/10.1016/j.molbiopara.2009.12.007

Singson A., 2001 Every Sperm Is Sacred: Fertilization in Caenorhabditis elegans. Developmental Biology 230. https://doi.org/10.1006/dbio.2000.0118

Taylor P, Brown JH. Synthesis, Storage and Release of Acetylcholine. In: Siegel GJ, Agranoff BW, Albers RW, et al., editors. Basic Neurochemistry: Molecular, Cellular and Medical Aspects. 6th edition. Philadelphia: Lippincott-Raven; 1999. Available from: https://www.ncbi.nlm.nih.gov/books/NBK28051/

Tian, L., Hires, S. A., Mao, T., Huber, D., Chiappe, M. E., Chalasani, S. H., Petreanu, L., Akerboom, J., McKinney, S. A., Schreiter, E. R., Bargmann, C. I., Jayaraman, V.,

Svoboda, K., & Looger, L. L. (2009) Imaging neural activity in worms, flies and mice with improved GCaMP calcium indicators. *Nature methods*, *6*(12), 875–881. https://doi.org/10.1038/nmeth.1398

Timmons L., and A. Fire, 1998 Specific interference by ingested dsRNA. Nature 395. https://doi.org/10.1038/27579

Touroutine, D., Fox, R. M., Von Stetina, S. E., Burdina, A., Miller, D. M., & Richmond, J. E. (2005). Acr-16 encodes an Essential subunit of the LEVAMISOLE-RESISTANT nicotinic receptor at the Caenorhabditis Elegans neuromuscular junction. *Journal of Biological Chemistry, 280*(29), 27013-27021. doi:10.1074/jbc.m502818200

Trang A, Khandhar PB. Physiology, Acetylcholinesterase. [Updated 2020 Jul 10]. In: StatPearls [Internet]. Treasure Island (FL): StatPearls Publishing; 2021 Jan-. Available from: https://www.ncbi.nlm.nih.gov/books/NBK539735/